TECHNICAL TRANSACTIONS 7/2018
MECHANICS
DOI: 10.4467/2353737XCT.18.108.8803
SUBMISSION OF THE FINAL VERSION: 22/06/2018

Aneta Szewczyk-Nykiel (anykiel@mech.pk.edu.pl)
Institute of Material Engineering, Cracow University of Technology

The microstructure and properties of titanium carbide reinforced stainless steel matrix composites prepared by powder metallurgy

Mikrostruktura i właściwości spiekanych kompozytów o osnowie stali nierdzewnej umacnianych cząstkami węglika tytanu

Abstract

TiC particle-reinforced AISI 316L stainless-steel matrix composites were prepared using conventional powder metallurgy technology. The effect of TiC content on the microstructure and properties of these composites has been investigated with a particular emphasis upon hardness, wear resistance and corrosion resistance in sea water environments. The results showed that TiC particle reinforcement improved the hardness, wear resistance and corrosion resistance of AISI 316L stainless steel. The higher TiC content in the studied composites resulted in a higher hardness of the wear surface and a lower wear rate. The best corrosion resistance in sea water was achieved for sintered AISI 316L – 5% TiC composite.

Keywords: metal matrix composites, TiC particles, AISI 316L, density, hardness, wear resistance, corrosion resistance, microstructure

Streszczenie

Konwencjonalną technologią metalurgii proszków wytworzono umacniane cząstkami TiC kompozyty o osnowie austenitycznej stali AISI 316L. Dokonano oceny wpływu udziału cząstek TiC na mikrostrukturę i właściwości tych kompozytów, w szczególności twardość, odporność na zużycie ścierne i odporność na korozję w środowisku wody morskiej. Stwierdzono, że umocnienie cząstkami TiC doprowadziło do poprawy twardości, odporności na zużycie ścierne i odporności na korozję stali AISI 316L. Wraz ze wzrostem udziału TiC w badanych kompozytach wzrastała twardość powierzchni zużycia, a malała jej szybkość. Natomiast najlepszą odporność na korozję w wodzie morskiej wykazał spiekany kompozyt AISI 316L – 5% TiC.

Słowa kluczowe: kompozyty o osnowie metalowej, cząstki TiC, AISI 316L, gęstość, twardość, odporność na zużycie ścierne, odporność na korozję, mikrostruktura

1. Introduction

Ceramic particle-reinforced metal matrix composites exhibit attractive physical and mechanical properties, such as high strength-to-density and stiffness-to-density ratios, hardness, thermal stability, good wear resistance and corrosion resistance. The possibility to use a ferrous alloy as a matrix in composites is of great practical importance. This particularly applies to steels. They are the most commonly used metallic structural materials that are commercially available in many grades. They are characterised by greater stiffness, strength and hardness in comparison to aluminium or its alloys, good machinability and weldability; furthermore, steels often exhibit better corrosion resistance [1–3].

The use of reinforcement in the form of ceramic particulates is beneficial for many reasons: its comparatively simpler and cheaper production procedures results in lower costs than other types of reinforcement; its ceramic particulates can greatly enhance mechanical and tribological properties; its use in composites results in high levels of resistance to corrosion [1, 4–12].

In general, steel matrix composites are reinforced with the following particles: carbides (SiC, TiC, WC), borides (TiB_2) and oxides (Al_2O_3, Y_2O_3) [1, 4–25]. Titanium carbide particles can be considered to be a suitable reinforcement for steel matrix composites due to their high hardness, low density, good wetting, chemical inertness, and high melting point [4, 13, 15, 16, 21–25].

The properties of metal matrix composites largely depend on the type and properties of the reinforcement particle material, the reinforcement volume fraction, as well as the size and shape of particles. It is considered that the optimal properties of such composites can be obtained in the case of small sizes of reinforcement particles made from material which exhibits high thermal stability and uniform particle distribution in the metal matrices of these composites [13, 18]. In the case of structural applications, MMCs with a low volume fraction of reinforcement (from 5% up to 30%) are typically used. When the product application requires high levels of hardness and wear resistance, the volume fraction of reinforcement can be as high as 50% or even 80% [18]. The ability of these composites to possess exceptional properties allows them to be used to produce wear- and corrosion-resistant parts of machines, devices, and even tools [14]. Particle-reinforced MMCs are produced using powder metallurgy technology, mechanical alloying, infiltration and casting [18].

Studies relating to the manufacturing of TiC-reinforced composites with matrices of tool steel and stainless steel can be found in the literature as can papers studying the effects of titanium carbide reinforcement on the microstructure, sintering kinetics, hardness and wear resistance of these composites [1, 4, 10, 11, 13–18, 21–25]. The microstructure and mechanical properties of 316L stainless steel matrix composites, sintered for 45 minutes in pure hydrogen at 1350°C, reinforced with different volume fractions of TiC particles (1.5 and 4 vol.%) have been studied [21, 22]. It was stated that the addition of carbide particles decreased the density of sintered materials although a transient liquid phase appeared during the sintering process. The UTS, yield strength and strain at break of 316L-TiC composites decreased with increasing TiC content, while hardness increased.

The wear resistance of 316L-TiC (2%, 5%, 10% and 15%) composites produced using conventional sintering as well as microwave sintering was investigated in [16]. It was found that

the best tribological properties (applied load of 100 N, sliding velocity of 0.5 m/s) combined with good densification were obtained for composites with the lowest content of TiC particles.

Article [17] deals with the investigation of the effect of the addition of reinforcement (TiC, Al_2O_3 and Y_2O_3 particles at the amounts of 4 wt.% to 6 wt.%.) on the mechanical properties and corrosion behaviour of austenitic stainless steel matrix composites, sintered at 1250°C for 20 minutes in a nitrogen atmosphere. It was stated that TiC-reinforced composites exhibited the highest values of hardness. Potentiodynamic polarisation measurements revealed that the addition of TiC improved the corrosion resistance of sintered austenitic stainless steel matrix composites in an environment of 3.5% NaCl. Moreover, corrosion rate decreased as the amount of TiC increased. Of all materials, the lowest value of corrosion rate was found for stainless steel – 6 wt.% TiC composite.

According to [11], the oxidation resistance of 316L matrix composites can be improved by the addition of TiC particles (due to the formation of Cr-ion-enriched oxide film). It was also stated that the reduction of the oxidation film densification and the deterioration of the oxidation performance took place in the composites with excessively high levels of TiC additions due to the agglomeration of particles.

It has also been confirmed that the addition of TiC particles can improve the mechanical properties of 316L steel matrix composites when the content of reinforcing particles is not too excessive. It was stated that 316L – 10% TiC composite exhibited the highest values of tensile strength (655.3 MPa) [23].

The aim of the present paper is to determine the influence of the addition of titanium carbide particles on the microstructure and properties of sintered AISI 316L austenitic stainless steel matrix composites. In particular, the focus is on the following properties: hardness, wear resistance (dry sliding friction), and corrosion resistance in an environment of natural sea water (originating from the Baltic Sea) and an artificial environment. Based on the review of literature and previous experience, the content of titanium carbide particles was selected. It was decided that 5% and 10% TiC would be added to the stainless steel powder.

2. Materials for research

In the present studies, commercial available powders of AISI 316L stainless steel provided by Höganäs and titanium carbide were used as the matrix and the particulate reinforcement. The chemical composition of AISI 316L is provided in Table 1. The average particle size is < 150 μm with 32 % participation of powder particles of sizes less than 45 μm. Titanium carbide with a purity of 99.5 % has an average particle size of 5 μm.

Table 1. Chemical composition of AISI 316L steel powder (wt.%)

Cr	Ni	Mo	Mn	S	C	Fe
17.5	13	2.2	0.1	0.8	0.02	Bal.

In order to compare the results, pure AISI 316L powders were also used in these studies.
The following powder mixtures were prepared:

- AISI 316L – 5 wt.% TiC,
- AISI 316L – 10 wt.% TiC.

3. Experimental procedure

Cylindrical samples of sizes ∅20×5 [mm] and ∅25.4×6 [mm] were produced during a process consisting of the preparation of powder mixtures, pressing and sintering. The mixtures of AISI 316L and TiC powders were prepared by dry mixing the components in a Turbula® mixer for six hours in an atmosphere of normal air. These powder mixtures, and also the AISI 316L powder, were then pressed in a rigid matrix at 700 MPa. The sintering process was performed in a Nabertherm furnace in a pure (99.9992 %) and dry (dew point below -60°C) hydrogen atmosphere. The flow rate of the gas was 100 ml/min. The temperature of the isothermal sintering was 1240°C. The sintering time was 60 minutes. The samples were slowly heated to the isothermal sintering temperature and cooled from sintering temperature to ambient temperature at a rate of 10°C/min.

The measurements of green density were performed using the geometrical method, while the density and open porosity of the sintered materials were measured using the water-displacement method (according to the demands of the PN-EN ISO 2738:2001 norm).

Metallographic cross sections were prepared. The microstructural study was conducted with a Nikon Eclipse ME 600P Light Optical Microscope (with digital image recording), and a Joel JSM550LV Scanning Electron Microscope. The microstructure of the studied materials was examined before and after etching. An EDS analysis was also performed.

The hardness measurements by the Rockwell method (B scale) were conducted according to the EN 24498-1: 1993 norm. The HV0.01 (10s) microhardness was determined using a FM 700 E microhardness tester.

Roughness measurements were performed using a Mitutoyo SurfTest SJ-301 surface roughness tester. The surface roughness parameters (R_a, R_z, R_q) were determined.

The wear resistance test was performed using a ITeE-PIB T-01M tribotester in accordance with ASTM G99-95A: 'Standard Test Method for Wear Testing with Pin-on-Disk Apparatus'. Steel 1.3505 with a hardness of 40 HRC was used as a counterbody. The various applied loads (10 N, 20 N) and sliding velocities (0.12 m/s, 0.2 m/s) were used. The sliding distance was 500 m. The friction coefficient as a function of the sliding distance was recorded. The average values of the friction coefficient, the absolute weight loss, the wear rate and the width of the wear paths on the surface of the samples were defined in order to evaluate the wear resistance of the studied composites under conditions of dry sliding friction.

Corrosion resistance tests including open-circuit potential and potentiodynamic polarisation measurements were performed using the ATLAS 0531 electrochemical unit & impedance analyzer (ATLAS – SOLLICH), controlled by AtlasCorr05 software. Corrosion behaviour of the studied materials was investigated in an environment of natural sea water

(originating from the Baltic Sea) as well as artificial sea water. A conventional three-electrode system consisting of the working electrode, the counter electrode (platinum electrode) and the reference electrode (saturated calomel electrode) was used. The working electrode was the sample of the studied materials: sintered AISI 316L – TiC composites and AISI 316L steel. The surface of the working electrode was ground, washed using distilled water, degreased in acetone and then dried in air.

At first, the open circuit potential as a function of immersion time (60 minutes) was measured, then potentiodynamic polarisation measurement was performed. A polarisation curve was obtained at a potential scan rate of 1.0 mV/s from – 0.8 V to + 0.6 V. The corrosion current density (i_{corr}), corrosion potential (E_{corr}), cathodic (b_c) and anodic (b_a) Tafel constants were determined based on the polarisation curve. The polarisation resistance (R_{pol}) was evaluated using the Stern method and the Stern-Geary method. According to standard ASTM G 102, corrosion rates, both in terms of the penetration rate (CR) and the mass loss rate (MR), were determined.

4. Results and discussion

The results of density measurements performed after pressing and the sintering process for AISI 316L-TiC composites and AISI 316L steel are shown in Fig. 1 on the basis of depending on the amount of titanium carbide introduced into the powder mixtures. Additionally, the density of AISI 316L-TiC composites which were determined according to the rule of mixture and values are plotted in the form of rhombus markers in Fig. 1; this was in order to compare the values of the theoretical density with the measured values. The results of open and closed porosity measurements for the same sintered materials are presented in Fig. 2.

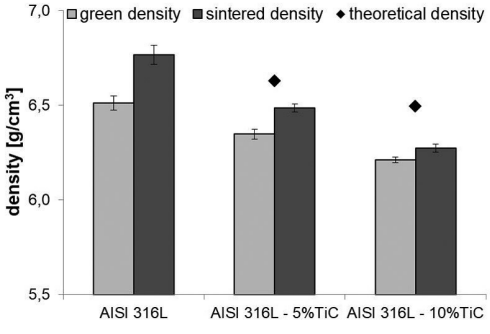

Fig. 1. The green and sintered densities of AISI 316L steel and AISI 316L-TiC composites

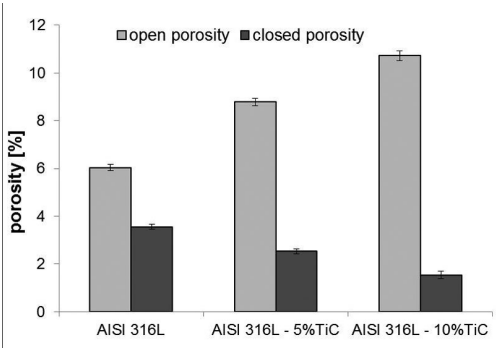

Fig. 2. The open and closed porosities of AISI 316L steel and AISI 316L-TiC composites

Based on the analysis of the results presented above, it can be concluded that the addition of titanium carbide contributed to the obtaining of lower values of green and sintered density of AISI 316L-TiC composites in comparison to AISI 316L stainless steel. In addition, it can be seen that the density of the studied composites after both the pressing and sintering processes

decreases with as the amount of titanium carbide added to the powder mixtures increases up to 10 wt. %. This behaviour is in accordance with the rule of mixture and it is caused by differences in the densities of the basic components of the studied composites. Specifically, the introduction of reinforcing particles made from a material with a lower density than the density of the matrix material leads to a reduction in the density of the composite. The effect of an increased number of reinforcing ceramic particles on the deterioration of sinterability was also found in the case of sintered Distaloy DC – SiC, Distaloy SA – SiC and Distaloy SE – SiC composites [9, 12]. Although the values of theoretical and experimental sintered density are different from each other, in the both cases, the dependence of density on the amount of titanium carbide introduced into the powder mixtures is the same, i.e. the higher the TiC content, the lower the sintered density of AISI 316L-TiC composites. Because the difference between the values of theoretical and experimental sintered densities increases with increasing titanium carbide content, it can be stated that too many TiC particles in the steel matrix inhibit the transport mechanisms; this leads to densification of the matrix material during sintering. This was confirmed by the values of the calculated densification parameter, which, in comparison to AISI 316L steel, are almost twice as low for AISI 316L – 5 wt.% TiC composite and a little more than three times as low for AISI 316L – 10 wt.% TiC composite. A clear influence of the composition on the porosity of studied materials can also be observed. The open porosity increases, while the closed porosity decreases with the increase of titanium carbide content in the composite. Ultimately, the total porosity slightly increases.

The microstructure of sintered AISI 316L steel and AISI 316L-TiC composites (before and after etching) are shown in Figs. 3–5. There are visible irregular pores that show a clear tendency to connect with each other in the microstructure of austenitic steel. These pores are unequally spaced across the observed surface. Etching revealed the clear grain boundaries of austenite with a microhardness of around 170 HV0.01.

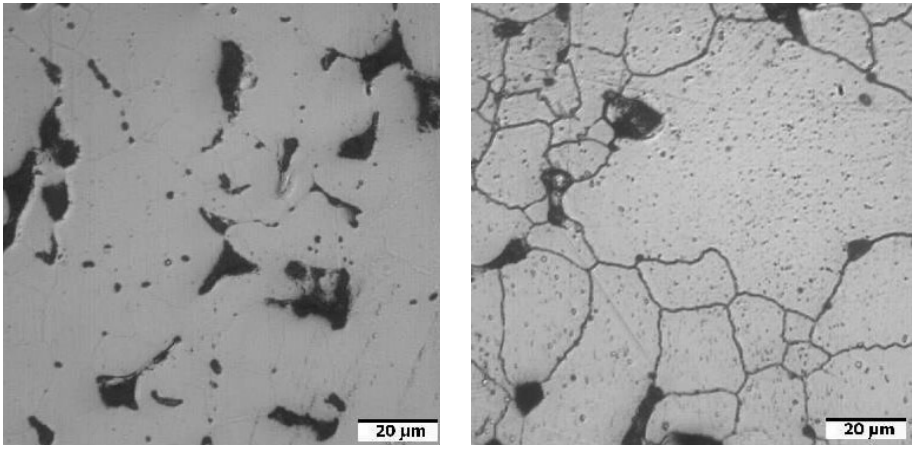

Fig. 3. The microstructure of sintered AISI 316L steel in the unetched (a) and etched (b) conditions

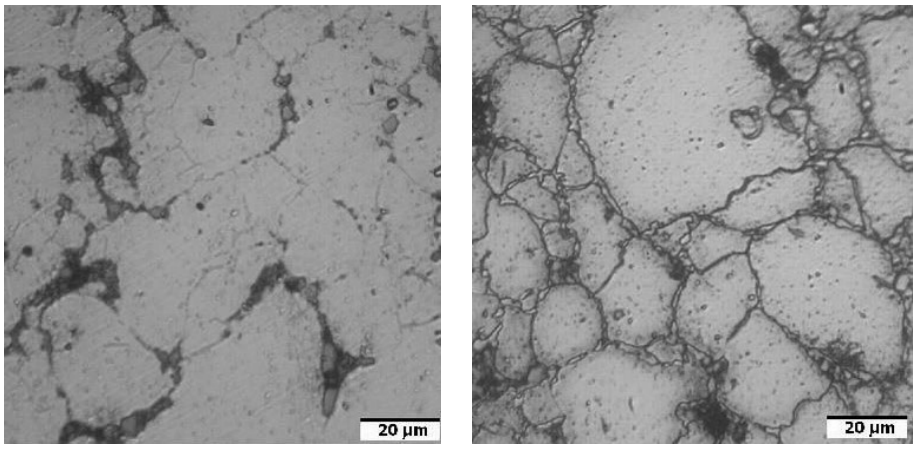

Fig. 4. The microstructure of sintered AISI 316L – 5 wt.% TiC composite in the unetched (a) and etched (b) conditions

As anticipated, the addition of titanium carbide induced a distinct change in the microstructure. While the pores observed in the microstructure of AISI 316L steel tend to connect to each other, in the case of the studied composites, the pores are visibly isolated. Admittedly, they have irregular shapes; however, their sizes are smaller. These pores are largely filled with small TiC particles, which determines their smaller size. Furthermore, titanium carbide particles have a clear tendency to concentrate on the grain boundaries of the matrix. Of course, as the amount of introduced titanium carbide is increased, the amount of reinforcing particles located on the grain boundaries also increases, so the nearly continuity of their occurrence can be noticed in AISI 316L – 10 wt.% TiC composite, because they form as though a net at the grain boundaries of the matrix meaning unclear due to grammatical errors, this needs. The titanium carbide particle size ranges from around 2 µm to 6 µm. The microhardness of the matrix increases from around 290 HV0.01 to around 380 HV0.01 with an increase in the amount of TiC added.

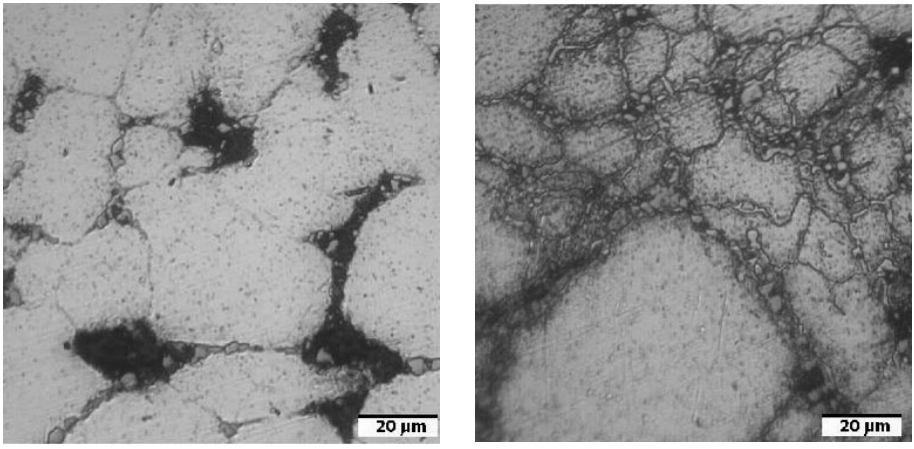

Fig. 5. The microstructure of sintered AISI 316L – 10wt. % TiC composite in the unetched (a) and etched (b) conditions

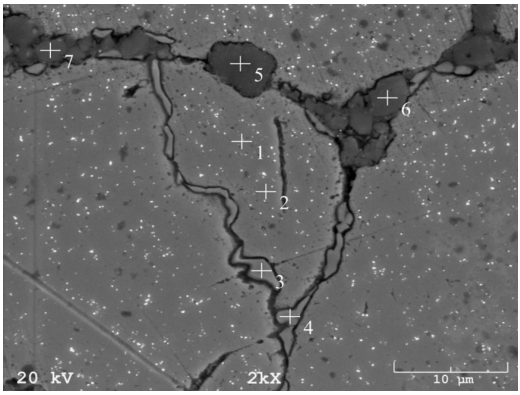

Fig. 6. The microstructure (SEM) of sintered AISI 316L – 5 wt.% TiC composite

It can be stated that the distribution of TiC particles in the matrix is insufficiently homogeneous. A slight agglomeration of fine TiC particles and formation of porous structure in the areas adjacent to these particles is visible in the microstructure of sintered AISI 316L-TiC composites.

The SEM microstructure of the sintered AISI 316L – 5 wt.% TiC composite is shown in Fig. 6. The results of the chemical composition microanalysis are presented in Table 2.

Elements such as Fe, Cr, Ni and Mo are present at points 1–4. These are the main elements of AISI 316L stainless steel chemical composition. The microanalysis of chemical composition at points 3 and 4 revealed a higher chromium content in comparison to the results obtained at points 1 and 2. It can be assumed that a σ phase appeared on the grain boundaries. As can be observed, points 5, 6 and 7 are located in the area of titanium carbide particles situated on the grain boundaries of the austenitic matrix. The main elements at these points are carbon and titanium although there are also trace of Fe, Cr, and Ni.

Table 2. The results of the microanalysis of chemical composition of sintered AISI 316L – 5 wt.% TiC composite (points are marked in Fig. 6)

Point number	**Chemical composition, wt.%**					
	Mo	Cr	Fe	Ni	C	Ti
1	1.68	17.30	69.34	11.68	–	–
2	1.89	17.49	69.25	11.37	–	–
3	0.81	36.97	53.01	9.21	–	–
4	0.94	30.06	59.25	9.76	–	–
5	–	0.36	0.65	0.26	35.76	62.94
6	–	0.41	0.71	0.31	35.64	62.93
7	–	0.38	0.69	0.29	35.72	62.92

There are different factors which affect wear resistance. These include applied load, sliding velocity, sliding distance, operating temperature and the type (or lack) of lubrication. Factors related to material properties should be also mentioned. In the case of composites, these properties are the type of matrix material, hardness of this material, and surface condition (roughness); in the case of reinforced particles, these properties are the type of material, their shape, size, distribution in the matrix and volume fraction.

The results of the measurements of HRB hardness and surface roughness for all the studied materials are presented in Figs 7 and 8, respectively.

As expected, the presence of hard titanium carbide reinforcing particles in the austenitic steel matrix resulted in a marked increase in the hardness of the sintered composites. It can be seen that the increase in the amount of titanium carbide in the range of 5 to 10 wt.% ensured the increase of the hardness of AISI 316L-TiC composites. By contrast, the values of all measured surface roughness parameters (R_a, R_z, R_q) decreased with increases in the amount of TiC particles in the studied composites.

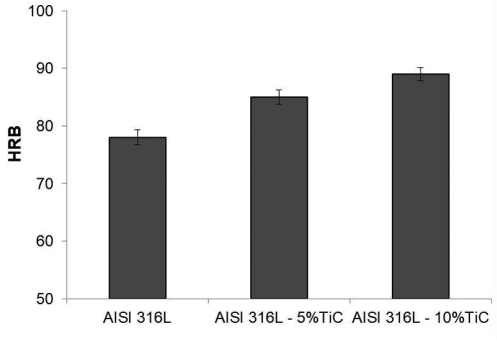

Fig. 7. Hardness of AISI 316L steel and AISI 316L-TiC composites

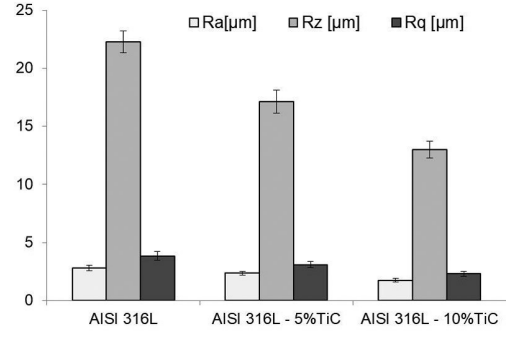

Fig. 8. Parameters of surface roughness of AISI 316L steel and AISI 316L-TiC composites

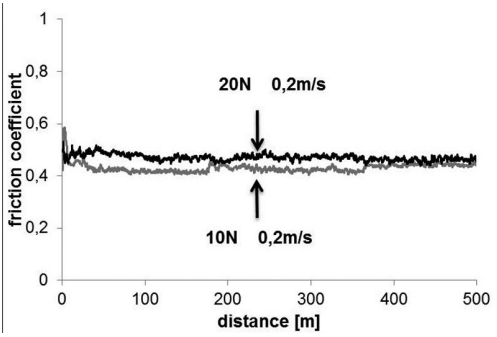

Fig. 9. Dependence of the friction coefficient on the sliding distance for sintered AISI 316L steel and AISI 316L-TiC composites during dry sliding friction conditions (applied load of 10N, sliding velocity of 0.2 m/s)

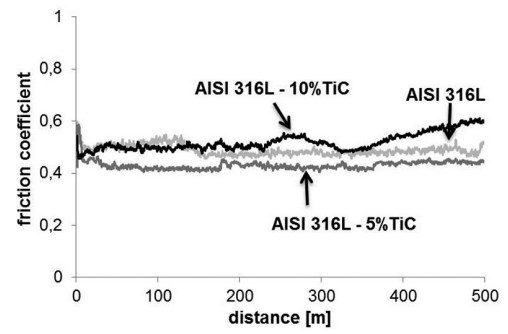

Fig. 10. Dependence of the friction coefficient on the sliding distance for sintered AISI 316L – 5 wt. % TiC composites during dry sliding friction conditions (constant sliding velocity of 0.2 m/s, different applied load)

Some examples of the recorded dependence of the friction coefficient on the sliding distance for AISI 316L steel and AISI 316L-TiC composites relating to dry sliding friction are presented in Figs. 9 and 10.

For all of the studied materials, the dependences of the friction coefficient on sliding distance show a distinct similarity. It can be observed that the value of the friction coefficient rapidly increases in the initial stage, then slightly decreases, and then stabilises until the end of the test. The abovementioned dependences cover the range from the break-in stage (up to about 100–150 m) to the steady-state wear stage.

The values of the friction coefficient, the absolute weight loss and the width of the wear paths on the sample surfaces of the AISI 316L steel and AISI 316L-TiC composites were determined and these are presented in Table 3. Figure 11 shows the variation of the wear rate of the studied materials.

Table 3. The values of the friction coefficient, the absolute weight loss and the width of the wear paths on the sample surfaces of the AISI 316L steel and AISI 316L-TiC composites

Material	Applied load [N]	Sliding velocity [m/s]	μ	Δm [g]	r [mm]
AISI 316L	10	0.12	0.457	0.012	1.326
		0.20	0.480	0.019	1.543
	20	0.12	0.468	0.030	1.764
		0.20	0.540	0.045	1.899
AISI 316L – 5%TiC	10	0.12	0.453	0.010	1.315
		0.20	0.462	0.014	1.436
	20	0.12	0.456	0.029	1.645
		0.20	0.476	0.035	1.828
AISI 316L – 10%TiC	10	0.12	0.474	0.002	1.229
		0.20	0.537	0.006	1.295
	20	0.12	0.583	0.009	1.249
		0.20	0.587	0.012	1.579

It can be stated that the introduction of titanium carbide had a favourable impact on the wear resistance of AISI 316L matrix composites. This was confirmed by lower values of the absolute weight loss, wear rate, and the width of the wear paths for composites compared to the values obtained for sintered AISI 316L steel. The increase of the sliding velocity at a constant value of applied load contributed to the increase of the values of the friction coefficient, the absolute weight loss and the width of the wear paths on the sample surface for all tested materials. Also, the increase of the applied load at a constant value of sliding velocity contributed to the increase of the values of the friction coefficient, the absolute weight loss and the width of the wear paths on the sample surface for all tested materials.

Regardless of the applied load and the sliding velocity, the wear rate of the AISI 316L-TiC composites is lower than that of the matrix material and, furthermore, it decreases with

increases to the TiC content. It can be observed that the wear rate of all studied materials increases with increasing applied and increases to sliding velocity.

It was observed that the higher content of titanium carbide particles in the studied composites resulted in a higher hardness of the wear surface and a lower wear rate. However, the AISI 316L – 10 wt.% TiC composite exhibited a higher value of friction coefficient with a lower absolute weight loss and wear rate in comparison to the AISI 316L – 5% TiC composite regardless of the applied load and sliding velocity. It can be concluded that there are some differences in the nature of wear resulting from different percentages of reinforcing particles in these composites. Lower values of mass loss can result from the mechanism of pulling out or crushing particles and pushing them into voids (open pores) that occur on the surface of the tested material samples.

Figure 12 presents the variation of open circuit potential with time (an environment of natural sea water) for sintered AISI 316L steel and AISI 316L-TiC composites. Generally, the OCP determines the thermodynamically tendency of a material to electrochemical corrosion reactions with a corrosive medium. The values of initial and final potentials (after 60 minutes of immersion in sea water) for the AISI 316L-TiC composites (presented in Table 4) are the lowest and highest potentials values, respectively. The opposite case occurs for sintered AISI 316L steel.

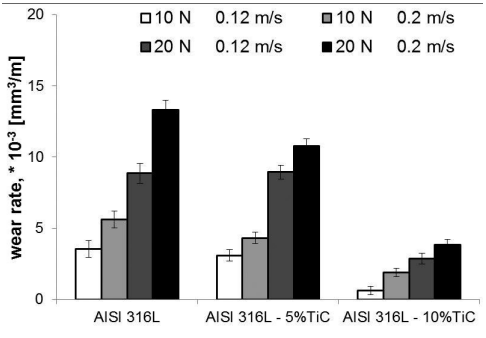

Fig. 11. Fig. 11. The effect of sintered AISI316L-TiC composites on TiC content on wear rate

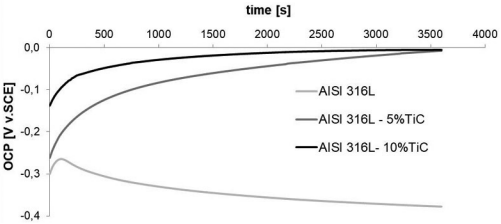

Fig. 12. Fig. 12. The variation of OCP with time for AISI 316L steel and AISI 316L-TiC composites (an environment of natural sea water)

A shift of the OCP in the direction of positive values over time can be observed in the case of AISI 316L-TiC composites. This suggests the formation of a passive layer on the sample surface. After some time, stabilisation takes place, which indicates the thermodynamic stability of the formed layer and its resistance to chemical degradation. This behaviour increases the corrosion resistance of the studied materials. Moreover, it can be stated that the AISI 316L-TiC composites show a higher corrosion resistance in an environment of natural sea water than the artificial environment.

The potentiodynamic polarisation curves of the sintered AISI 316L steel and AISI 316L-TiC composites relating to the natural and artificial sea water environments are shown in Figs. 13 and 14, respectively. As can be observed, the investigated materials do not exhibit a typical anodic polarisation curve containing an active, a passive and a transpassive region; there is

not a standard maximum of active-passive transition. The increase of current density occurs and destruction of passive layer proceeds, pitting corrosion appears.

There are many factors that influence corrosion resistance; the properties of the material and the characteristics of the environment being the most important. In the case of sintered materials, porosity affects the corrosion resistance. The undesirable effect of pores is attributed to large internal surface areas of sintered materials in products and a lack of passivation within the pores.

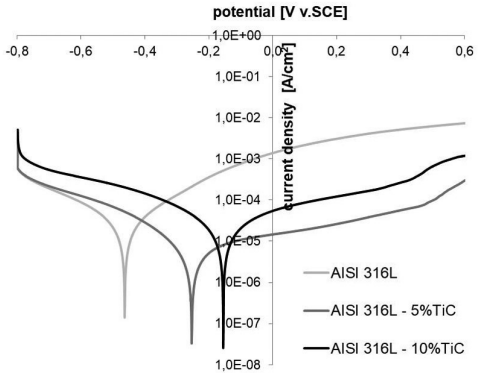

Fig. 13. Potentiodynamic polarisation curves of sintered AISI 316L steel and AISI 316L-TiC composites (environment of natural sea water)

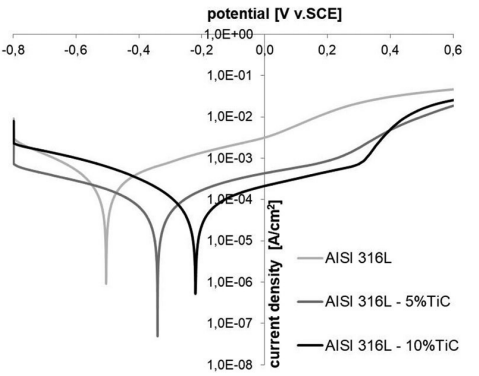

Fig. 14. Potentiodynamic polarisation curves of sintered AISI 316L steel and AISI 316L-TiC composites (environment of artificial sea water)

Table 4 lists the values of OCP, polarisation resistance (R_{pol}), corrosion potential (E_{corr}), corrosion current density (i_{corr}), anodic (b_a) and cathodic (b_c) Tafel constants, and corrosion rate (CR and MR) of the investigated materials immersed in natural and artificial sea water.

It is obvious that the corrosion resistance of the studied materials depends on several factors including material composition and the type of corrosive environment. Based on the analysis of the results presented above, it can be concluded that parameters such as polarisation resistance, corrosion current density and corrosion rate achieved more favourable values in the case of the natural sea water environment than for the artificial environment. The addition of titanium carbide as reinforcement improved the corrosion resistance of the AISI 316L austenitic stainless steel in both of the tested environments. However, an increase in the amount of reinforcing particles from 5 to 10 wt.% was not beneficial because it led to a lower value of polarisation resistance and an increase in the corrosion current density and the corrosion rate. In the environment of both natural and artificial sea water, the sintered AISI 316L – 5 wt.% TiC composite obtained the highest value of the polarisation resistance and the lowest values of corrosion current density and corrosion rate. This means that this material has the highest corrosion resistance.

Table 4. The values of open circuit potential (initial and final), polarisation resistance (R_{pol}), corrosion potential (E_{corr}), corrosion current density (i_{corr}), anodic (b_a) and cathodic (b_c) Tafel constants, and corrosion rate (*CR* and *MR*) for sintered AISI 316L stainless steel and AISI 316L-TiC composites

Material	AISI 316L	AISI 316L – 5 wt.% TiC	AISI 316L – 10 wt.% TiC
	Natural sea water		
OCP_{START} [V]	-0.300	-0.262	-0.138
OCP_{STOP} [V]	-0.377	-0.008	-0.005
R_{pol} [Ω cm²] [1)]	1704	8673	2507
R_{pol} [Ω cm²] [2)]	2198	12464	3479
E_{corr} [V]	-0.463	-0.254	-0.155
i_{corr} [A cm^{-2}]	1.74E-05	3.93E-06	1.64E-05
b_a [V]	0.178	0.304	0.305
b_c [V]	0.173	0.180	0.232
CR [mm/year]	0.021	0.005	0.019
MR [g/cm²d]	0.388	0.081	0.330
	Artificial sea water		
OCP_{START} [V]	-0.313	-0.280	-0.163
OCP_{STOP} [V]	-0.393	-0.131	-0.104
R_{pol} [Ω cm²] [1)]	222	879	867
R_{pol} [Ω cm²] [2)]	294	1324	1222
E_{corr} [V]	-0.504	-0.220	-0.341
i_{corr} [A cm^{-2}]	2.54E-04	4.86E-05	4.97E-05
b_a [V]	0.432	0.310	0.281
b_c [V]	0.285	0.284	0.279
CR [mm/year]	0.300	0.057	0.060
MR [g/cm²d]	5.097	1.006	1.112
[1)] Stern method [2)] Stern-Geary method			

5. Conclusion

AISI 316L stainless steel matrix composites reinforced with TiC particles were manufactured using commercially available powder grades and conventional powder metallurgy technology. Based on the analysis of the presented results, it can be concluded that the microstructure and properties of sintered AISI 316L-TiC composites, such as wear resistance and corrosion resistance, are strongly dependent on the composition of the powder mixture.

The microstructure studies revealed a slight agglomeration of fine TiC particles and a clear tendency for these particles to be concentrated on the grain boundaries of the matrix, and the formation of a porous structure in the areas adjacent to these particles.

The presence of TiC particulate reinforcement caused a reduction in the density of AISI 316L-TiC composites after both the pressing and sintering processes in comparison to the matrix material. The density decreased with increasing amounts of TiC in the composite. This phenomenon is well known and it is caused by the introduction of an additive with a lower density into a matrix with a higher density. Moreover, the addition of TiC particles impedes

material densification during sintering and a lower relative density and higher porosity were obtained for the sintered AISI 316L-TiC composites in comparison to AISI 316L steel.

A Rockwell hardness test showed that the addition of titanium carbide as reinforcement to AISI 316L austenitic steel resulted in a marked increase in the hardness of the sintered composites. The hardness of the AISI 316L-TiC composites increased with the increase in the amount of TiC in the range from 5 to 10 wt.%. The hardness increase is caused by the material microstructural changes, mainly due to the presence of particles (made from hard titanium carbide) in the matrix.

The introduction of titanium carbide particles as reinforcement has a favourable affect upon the wear resistance of studied composites. This was confirmed by lower values of friction coefficient, the absolute weight loss and the wear rate obtained for the AISI 316L-TiC composites compared to the matrix material.

Based on the analysis of the potentiodynamic measurement results, it can be concluded that the addition of titanium carbide as reinforcement to the austenitic steel matrix composites improved the corrosion resistance in both tested environments. However, the increase of TiC content from 5 to 10 wt.% led to a decrease of polarisation resistance, and an increase of current density and corrosion rate. The sintered AISI 316L – 5 wt.% TiC composite exhibited the highest value of polarisation resistance and the lowest values of current density and corrosion rate in both the natural and the artificial sea water environments. This confirms that this material has the highest corrosion resistance.

References

[1] Sulima I., Klimczyk P., Hyjek P., *The influence of the sintering conditions on the properties of the stainless steel reinforced with TiB_2 ceramics*, Archives of Materials Science and Engineering, 39, 2009, 103–106.

[2] Kurgan N., *Effects of sintering atmosphere on microstructure and mechanical property of sintered powder metallurgy 316L stainless steel*, Materials and Design, 52, 2013, 995–998.

[3] Pandya S., Ramakrishna K.S., Annamalai R.A., Upadhyaya A., *Effects of sintering temperature on the mechanical and electrochemical properties of austenitic stainless steel*, Materials Science & Engineering A, 556, 2012, 271–277.

[4] Popoola A.P.I., Obadele B.A., Popoola O.M., *Effects of TiC–Particulate Distribution in AISI 304L stainless steel matrix*, Materials Digest Journal of Nanomaterials and Biostructures, 7, 2012.

[5] Sulima I., *Tribological Properties of Steel/TiB_2 Composites Prepared by Spark Plasma Sintering*, Archives of Materials Science and Engineering, 59, 2014, 1264–1268.

[6] Padmavathi C., Upadhyaya A., Agrawal D., *Corrosion behavior of microwave-sintered austenitic stainless steel composites*, Scripta Materialia, 57, 2007, 651–654.

[7] Nahme H., Lach E., Tarrant A., *Mechanical property under high dynamic loading and microstructure evaluation of a TiB_2 particle-reinforced stainless steel*, Journal of Materials Science, 44, 2009, 463–468.

[8] Sulima I., Homa M., Malczewski P., *High-temperature corrosion resistance of steel–matrix composites*, Metallurgy and Foundry Engineering, 41(2), 2015, 71–84.
[9] Szewczyk–Nykiel A., *Microstructure and properties of sintered metal matrix composites reinforced with SiC particles*, Technical Transactions, 6/2017, 179–190.
[10] Lin S.J., Xiong W.H., Wang S.Y., Shi Q.N., *Effect of reinforcing particles content on properties of TiC/316L composites*, Materials Science and Engineering of Powder Metallurgy, 18(3), 2013, 373–378.
[11] Lin S.J., Xiong W.H., Shi Q.N., Wang S.Y., *Effect of TiC addition on oxidation behavior of TiC/316L composites and its mechanism*, Chinese Journal of Nonferrous Metals, 23(11), 2013, 3121–3126.
[12] Öksüz K., Kumruoğlu L., Tur O., *Effect of Sic_p on the Microstructure and Mechanical Properties of Sintered Distaloy DC Composites*, "Procedia Materials Science", 11/2015, 49–54.
[13] Akhtar F., Guo S.J., *Microstructure, mechanical and fretting wear properties of TiC-stainless steel composites*, Materials Characterization, 59, 2008, 84–90.
[14] Pagounis E., Lindroos V.K., *Processing and properties of particulate reinforced steel matrix composites*, Materials Science and Engineering A, 246, 1998, 221–234.
[15] Shaojiang L., Weihao X., *Corrosion Behaviour of Powder Metallurgy Processed TiC/316L Composites with Mo Additions*, The Minerals, Metals & Materials Society, 67(6), 2015, 1362–1369.
[16] Shaojiang L., Weihao X., *Microstructure and abrasive behaviors of TiC–316L composites prepared by warm compaction and microwave sintering*, Advanced Powder Technology, 23, 2012, 419–425.
[17] Hegde A., Patil A., Tambrallimath V., *Corrosion Behaviour of Sintered Austenitic Stainless Steel Composites*, International Journal of Engineering Research & Technology, 3, 2014, 14–17.
[18] Akhtar F., *Ceramic reinforced high modulus steel composites: processing, microstructure and properties*, Canadian Metallurgical Quaeterly, 53(2), 2014, 253–263.
[19] Sulima I., Kowalik R., *Corrosion behaviors, mechanical properties and microstructure of the steel matrix composites fabricated by HP–HT method*, Materials Science & Engineering A, 639, 2015, 671–680.
[20] Sulima I., Klimczyk P., Malczewski P., *Effect of TiB_2 Particles on the Tribological Properties of Stainless Steel Matrix Composites*, Acta Metallurgica Sinica, 27(1), 2014, 12–18.
[21] Mima S., Yotkaew T., Morakotjinda M., Tosangthum N., Daraphan A., Karataitong R., Coovattanachai O., Vetayanugul B., Tongsri R., *Carbide–Reinforced 316L Composite*, The Fourth Thailand Materials Science and Technology Conference, Pathum Thani, Thailand, 31 March–1 April 2006.
[22] Coovattanachai O., Mima S., Yodkaew T., Krataitong R., Morkotjinda M., Daraphan A., Tosangthum N., Vetayanugul B., Panumas A., Poolthong N., Tongsri R., *Effect of admixed ceramic particles on properties of sintered 316L stainless steel*, Advances in Powder Metallurgy and Particulate Materials, 7, 2006, 161–171.
[23] Chakthin S., Poolthong N., Thavarungkul N., Tongsri R., *Iron–Carbide Composites Prepared by P/M*, Processing Materials for Properties, 2009, 577–584.

[24] Chakthin S., Morakotjinda M., Yodkaew T., Torsangtum N., Krataithong R., Siriphol P., Coovattanachai O., Vetayanugul B., Thavarungkul N., Poolthong N., Tongsri R., *Influence of Carbides on Properties of Sintered Fe–Base Composites*, Journal of Metals, Materials and Minerals, 18(2), 2008, 67–70.
[25] Xiong W., Lin S., *Microstructure and abrasive behaviors of TiC-316L composites prepared by warm compaction and microwave sintering*, Advanced Powder Technology, 23(3), 2012, 419–425.

If you want to quote this article, its proper bibliographic entry is as follow: Szewczyk-Nykiel A., *The microstructure and properties of titanium carbide reinforced stainless steel matrix composites prepared by powder metallurgy* , Technical Transactions, Vol. 7/2018, pp. 191–206.